Acta Pharmacologica Sinica

www.nature.com/aps

ARTICLE

Atypical chemokine receptor 3 induces colorectal tumorigenesis in mice by promoting β-arrestin-NOLC1-fibrillarin-dependent rRNA biogenesis

Juan Yang[1,2], Rong-rong Miao[3], Ya-nan Li[1], Ting Pan[1], Shu-hua Wu[4], Xian-jun Qu[3] and Shu-xiang Cui[1]

Atypical chemokine receptor 3 (ACKR3) has emerged as a key player in various biological processes. Its atypical "intercepting receptor" properties have established ACKR3 as the major regulator in the pathophysiological processes in many diseases. In this study, we investigated the role of ACKR3 activation in promoting colorectal tumorigenesis. We showed that ACKR3 expression levels were significantly increased in human colon cancer tissues, and high levels of ACKR3 predicted the increased severity of cancer. In Villin-ACKR3 transgenic mice with a high expression level of CKR3 in their intestinal epithelial cells, administration of AOM/DSS induced more severe colorectal tumorigenesis than their WT littermates. Cancer cells of Villin-ACKR3 transgenic mice were characterised by the nuclear β-arrestin-1 (β-arr1)-activated perturbation of rRNA biogenesis. In HCT116 cells, cotreatment with CXCL12 and AMD3100 selectively activated ACKR3 and induced nuclear translocation of β-arr1, leading to an interaction of β-arr1 with nucleolar and coiled-body phosphoprotein 1 (NOLC1). NOLC1, as the phosphorylated protein, further interacted with fibrillarin, a conserved nucleolar methyltransferase responsible for ribosomal RNA methylation in the nucleolus, thereby increasing the methylation in histone H2A and promoting rRNA transcription in ribosome biogenesis. In conclusion, ACKR3 promotes colorectal tumorigenesis through the perturbation of rRNA biogenesis by the β-arr1-induced interaction of NOLC1 with fibrillarin.

Keywords: tumorigenesis; ACKR3; NOLC1; fibrillarin; ribosome biogenesis; Villin-ACKR3 transgenic mice

Acta Pharmacologica Sinica (2022) 43:2967–2976; https://doi.org/10.1038/s41401-022-00901-x

INTRODUCTION

The chemokine receptor ACKR3, also known as CXCR7, is an atypical G protein-coupled receptor (GPCR) characterised by "intercepting receptor" signalling [1–3]. Unlike classical GPCRs, ACKR3 usually fails to activate canonical Gi protein-mediated signalling due to the lack of a conserved DRYLAIV structure [4]. ACKR3 was once regarded as a scavenger receptor and decoy receptor [5, 6]. ACKR3 can be activated by a number of endogenous ligands, including CXCL12, leading to many pathophysiological processes, including chronic inflammation, inflammation-driven tumorigenesis, tumour metastasis, chronic neurodegenerative disorders of the central nervous system, and even embryogenesis [7–9]. Mechanistically, upregulating ACKR3 accelerates pathophysiological processes by activating Akt/Keap-1/Nrf2 signalling and the PI3K-Akt pathway [10, 11]. To date, we do not have a complete understanding of how activated ACKR3 signalling is integrated to induce tumorigenesis.

Previously, we reported that as a "crosslinker" receptor, ACKR3 is likely to bind with CXCR4, a classic chemokine receptor for CXCL12 [12, 13], to form the ACKR3/CXCR4 heterodimer [14]. Upregulating ACKR3 exacerbated CXCR4-induced inflammation-driven colorectal tumorigenesis by increasing monocytic myeloid-derived suppressor cells and M2-like macrophages in the colorectal epithelium and lamina propria [14]. However, both ACKR3 and CXCR4 also responded to CXCL12 stimulation to induce chronic inflammation and colorectal tumorigenesis alone. Villin-ACKR3 mice demonstrated more advanced colorectal cancer (CRC) than Villin-CXCR4 mice under AOM/DSS induction. When CXCR4's contribution was prevented by AMD3100, the CXCR4 inhibitor Villin-CXCR7-CXCR4 mice still developed a large number of colonic tumours, indicating the main role of ACKR3 in colorectal tumorigenesis [14].

In this study, we uncovered a new mechanism by which ACKR3 induces tumorigenesis through β-arrestin-1-activated NOLC1 to perturb rRNA biogenesis in colon epithelial cells. Since β-arr2 has a strong nuclear export signal (NES) in its C-terminus, this specific NES excludes it from its sustained presence in the nucleus [15]. Thus, we identified β-arr1 as a downstream signalling pathway of activated ACKR3 in the pathophysiological processes of colorectal tumorigenesis. ACKR3-activated β-arr1 translocates into the nucleus to interact with NOLC1, a highly phosphorylated protein composed of N- and C-terminal domains and a unique central repeated domain consisting of alternating acidic and basic amino acid clusters localised in the nucleolus [16, 17]. Our results revealed that phosphorylated NOLC1 further interacted with fibrillarin, an rRNA methyltransferase [18, 19], to promote fibrillarin levels in the nucleolus and increase rRNA transcription

[1]Beijing Key Laboratory of Environmental Toxicology, Department of Toxicology and Sanitary Chemistry, School of Public Health, Capital Medical University, Beijing 100069, China; [2]Department of Comprehensive Ward, Affiliated Hospital of Guizhou Medical University, Guiyang 550004, China; [3]Department of Pharmacology, School of Basic Medical Sciences, Capital Medical University, Beijing 100069, China and [4]Department of Pathology, Hospital of Bin Zhou Medical College, Binzhou 256603, China
Correspondence: Shu-xiang Cui (cuisx@ccmu.edu.cn)

Received: 16 November 2021 Accepted: 13 March 2022
Published online: 1 April 2022

during ribosome biogenesis by upregulating methylation of histone H2A. We envision that future approaches to treating CRC should use ACKR3 inhibitors to block the ACKR3-activated nuclear translocation of β-arr1 to interact with NOLC1 and fibrillarin in the nucleolus.

MATERIALS AND METHODS

TCGA dataset

We referenced the microarray databases Oncomine (http://www.oncomine.org) and GEPIA (http://gepia.cancer-pku.cn) to analyse the levels of ACKR3 and NOLC1 in cancer tissues and normal tissues. To analyse the dataset, thresholds were set as follows: *P value*: 0.01; fold change: 2; gene rank: 20%; analysis type: cancer vs. normal; data type: mRNA.

Human colonic cancer specimens

The Ethics Committee of Binzhou Medical College approved this study to use human cancer samples. Human CRC specimens and paired nonneoplastic tissues ($n = 60$), including fresh CRC specimens ($n = 20$), were collected from resected specimens between February and May 2018 at Binzhou Medical College Hospital (Binzhou, China).

Human colonic cancer cell lines, cell culture and treatment

The human cancer cell lines SW480, SW620, HCT116, and HT29 and the normal colonic cell line NCM460 were purchased from the China Cell Bank authorised by American Type Culture Collection. Cells were cultured in DMEM (Gibco) containing 10% FBS (Gibco) at 37 °C in a humid atmosphere (5% CO_2). Cells were exposed to 40 ng/ml SDF-1α (CXCL12) (PeproTech) to activate ACKR3 or 10 μM AMD3100 (Selleck) to inhibit ACKR3 expression. The viability of cell growth was evaluated by the MTT assay as described elsewhere.

Villin-ACKR3 mice and the establishment of a colorectal cancer model

Villin-ACKR3-IREF mice expressing high ACKR3 in their intestinal epithelial cells (IECs) were generated by Cyagen Biosciences Inc. (Guangzhou, China). Villin-ACKR3-IREF mice and their WT littermates were maintained under controlled room temperature and allowed unrestricted access to standard mouse feed. Animal experiments were approved by the Animal Welfare Committee of Capital Medical University (AEEI-2016043). A mouse model of CRC was established as previously described [14, 20].

Histopathology and immunohistochemical staining assay

Routine haematoxylin-eosin staining (H&E staining) was performed to analyse cancer tissues. Immunohistochemical staining assays (IHC) were performed using antibodies against ACKR3 (Abcam), PCNA (Proteintech Group), and NOLC1 (Proteintech Group). IHC scoring was obtained based on the staining intensity and percentage of stained cancer cells as described elsewhere.

RNA interference assay

Small interfering RNA (siRNA) was designed by GenePharma (Suzhou, China). Human siACKR3, siβ-arr1, and siNOLC1 were cotransfected into the cells using Lipofectamine 2000 (Invitrogen) (the siRNA sequences are detailed in Table S1). Cells were plated in six-well plates for 24 h before interfering. The diluted Lipofectamine 2000 was lightly mixed with an equal volume of siRNA suspension. Each sample was incubated at room temperature for 20 min. The siRNA-lipid complex was added and incubated at 37 °C for 6 h. New medium was replaced, and the cells were incubated for 48 h before treatment.

RNA extraction and quantitative PCR (real-time PCR) assay

Total RNA was extracted by using TRIzol reagent according to the manufacturer's protocols (Invitrogen). For reverse transcription of total RNA, first-strand cDNA was synthesised with a ReverTra Ace® qPCR RT Kit (TOYOBO, Japan). Quantitative PCR was performed in triplicate using SYBR® Green Real-time PCR Master Mix (TOYOBO, Japan) on an ABI 7500 Real-Time PCR System. β-actin (ATCB) was used as an endogenous control, and fold changes were calculated by means of relative quantification ($2^{-\Delta\Delta}$CT). The primers used for quantitative PCR are listed in Table S2.

Western blotting and coimmunoprecipitation (Co-IP) assays

Western blotting assays were routinely performed. The primary antibodies are listed in Table S3. A co-IP assay was performed as described [21]. The antibodies included NOLC1 polyclonal antibody (Proteintech Group), β-arrestin-1 monoclonal antibody (Invitrogen) and fibrillarin antibody (Santa Cruz). Membranes were incubated with HRP-conjugated anti-rabbit IgG or HRP-conjugated anti-mouse IgG for 1 h at room temperature. Antibody-reactive proteins were detected by western chemiluminescent HRP substrate (ECL) (Millipore). Images were acquired by a FluorChem FC3 image analyser (Molecular Devices).

AgNOR staining analysis

AgNOR staining was performed as described [22, 23]. Paraffin deparaffinized sections were washed for 10 min and then stained in AgNOR Stain solution (Solarbio, China) at room temperature for 40–60 min. After rinsing in distilled water for 1–2 min, slides were counterstained for 1–3 min in methyl green staining solution, washed and finally air dried. AgNOR staining was analysed by the area quantification module of HALO v3.0.311.407 (Indica Labs) software.

Transmission electron microscopy (TEM)

Cancer cells were aspirated into the centrifuge tube and centrifuged at 800 *rpm* for 5 min. Cell pellets were fixed with 2.5% glutaraldehyde (Servicebio, China) for 2 h at 4 °C. Cell pellets were rinsed and fixed with 1% osmium tetroxide for 1 h. After dehydration through a graded ethanol series, samples were embedded in propylene oxide and resin (1:1). Sections were examined under a transmission electron microscope (JEM-2100, Japan).

Statistical analysis

Data are described as the mean ± SEM. Statistical analysis was performed with GraphPad Prism 8. Student's *t* test was used to compare differences between two groups. Statistical differences among multiple groups were analysed by one-way analysis of variance (ANOVA) followed by post hoc test with Dunnett (multiple comparisons to the same control). $P < 0.05$ was considered significant.

RESULTS

High expression of ACKR3 in human CRC specimens

To investigate the role of ACKR3 in CRC, we first analysed ACKR3 gene expression data issued in the Oncomine database. An analysis of a Hong Colorectal dataset indicated that the mRNA levels of ACKR3 were significantly higher in CRC tissues than in normal tissues ($P = 7.50 \times 10^{-5}$, fold change = 2.427) (Fig. 1a). Importantly, the increased ACKR3 was strongly associated with the progression of clinical stages of CRC, as indicated in the GEPIA database (Fig. 1b). F value = 2.23, Pr (>F) = 0.084. We then performed an immunohistochemistry (IHC) assay to analyse ACKR3 levels in human CRC tissues and paired paracancerous tissues (Fig. 1c). Of the 60 CRC specimens, 57 cases had higher levels of ACKR3 than their paracancerous tissues (Table S4). Western blotting assays identified higher levels of ACKR3 in fresh colon cancer tissues than in paracancerous tissues (Fig. 1d). In cultured cells, the colon cancer cell lines but not the normal colon cell line demonstrated higher levels of ACKR3 (Fig. 1e).

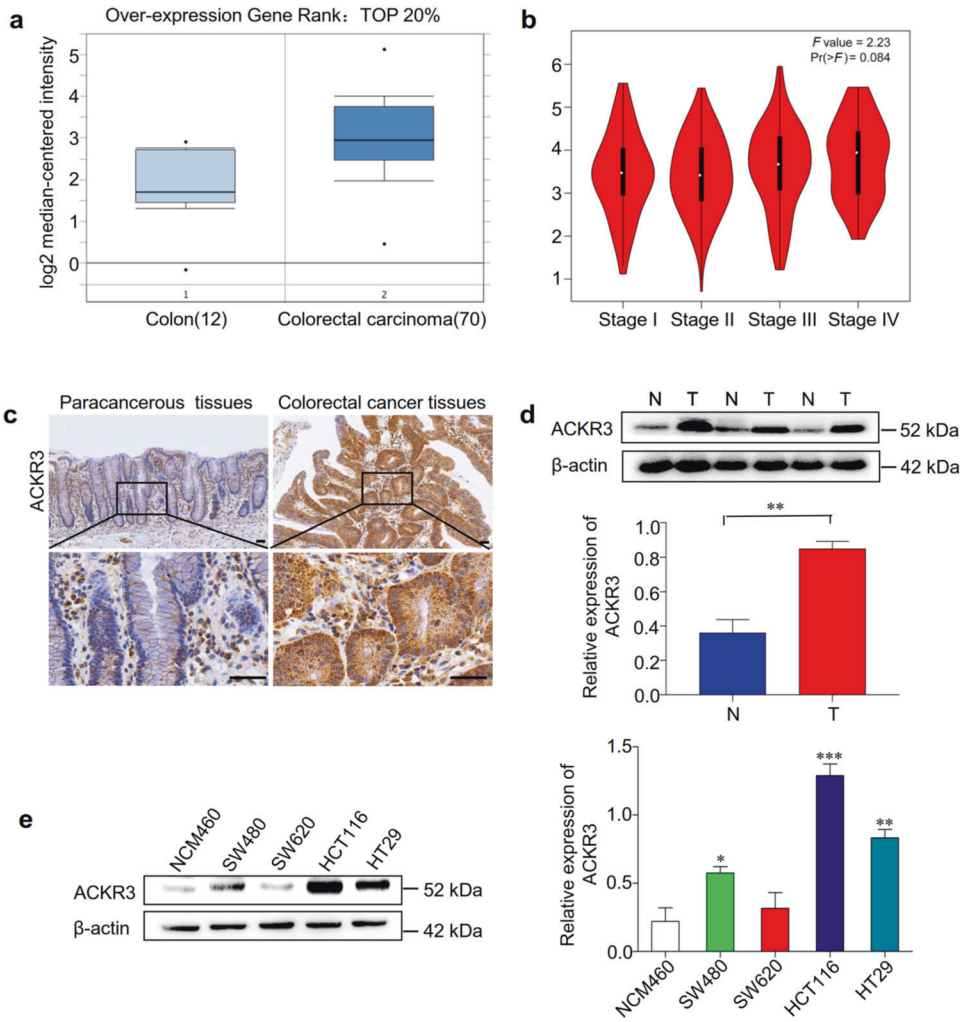

Fig. 1 Human CRC specimens expressed high ACKR3 levels. a Level of ACKR3 mRNA copy number in colorectal carcinoma and normal colonic tissue in the Hong Colorectal dataset. **b** Levels of ACKR3 varied in different stages of colorectal cancer. **c** Comparison of ACKR3 levels in CRC tissues and paired noncancer tissues. Upper images 10×, lower images 40×. The boxed region in each top panel is magnified and shown in the corresponding bottom panel. (10×) scale bar: 200 μm, (40×) scale bar: 50 μm. $n = 20$. **d** Western blotting of ACKR3 in human CRC tissues (T) and their paracarcinoma tissues (N) ($n = 20$). **e** Levels of ACKR3 in human colonic cancer cell lines and normal colonic epithelial cells. $^{*}P < 0.05$, $^{**}P < 0.01$, $^{***}P < 0.001$ vs. normal colonic tissue or normal colonic cell lines.

Intestinal epithelial cells of Villin-ACKR3 mice conferred the development of colorectal tumorigenesis

Villin-ACKR3 mice exhibited exacerbated colitis and colitis-associated tumorigenesis compared to their WT littermates, showing significant weight loss (Fig. 2a) and a high disease activity index (DAI index) (Fig. 2b). Villin-ACKR3 mice had shorter colorectal lengths than WT mice (Fig. 2c, d). Villin-ACKR3 mice developed more colorectal tumours than WT mice (Fig. 2e). Furthermore, colorectal tumours in Villin-ACKR3 mice demonstrated higher levels of ACKR3 (Fig. 2f) and CXCL12 (Fig. 2g) than those in their WT littermates. Microscopic analysis of colonic tissues showed exacerbated colonic damage with higher dysplasia in Villin-ACKR3 mice than in WT littermates (Fig. 2h). In addition, the levels of PCNA, CyclinD1, Caspase3, OCT4, SOX2, ALDH1, PTEN, c-Myc, ERK1/2, P-ERK1/2, mTOR, P-mTOR, AKT, and P-AKT were significantly higher in the colonic cancer cells of Villin-ACKR3-AD mice than in the colonic cancer cells of WT-AD mice (Fig. S1, $P < 0.01$). Villin-ACKR3-AD mice demonstrated elevated levels of inflammatory factors in the NF-κB/IL-6/STAT3 cascades, indicating ACKR3-induced colitis and colitis-associated tumorigenesis (Fig. S2, $P < 0.01$).

Activation of ACKR3 induced β-arr1 translocation into the nucleus to interact with nuclear NOLC1

As a downstream signal of GPCR, β-arr1 might respond to activated ACKR3. Colon cancer HCT116 cells exposed to CXCL12 demonstrated an increase in β-arr1 in the nucleus in a time-dependent manner ($P < 0.05$ vs. 0 h) (Fig. 3a). Since CXCL12 is the ligand of both ACKR3 and CXCR4, we used AMD3100, a specific CXCR4 inhibitor, to prevent CXCL12-activated CXCR4 from affecting ACKR3 and then analysed the expression level of β-arr1 in the nucleus. An increase in β-arr1 remained in the nucleus in the absence of CXCR4 (Fig. 3b). Nuclear β-arr1 was clearly seen in the immunofluorescence-stained cells (Fig. 3c). Nuclear β-arr1 was further observed in CRC cells of Villin-ACKR3 mice (Fig. 3d). Conversely, silencing ACKR3 prevented the translocation of β-arr1 into the nucleus (Fig. 3e). Silencing ACKR3 in HCT116 cells blocked CXCL12-stimulated growth (Fig. 3f), suggesting that upregulating ACKR3 accounts for the exacerbated tumorigenesis in colon cancer.

As β-arr1 was translocated into the nucleus, we next explored the functions of nuclear β-arr1. We searched any information regarding the interaction of β-arr1 with nuclear proteins issued in the HitPredict database. We observed a specific indication that β-

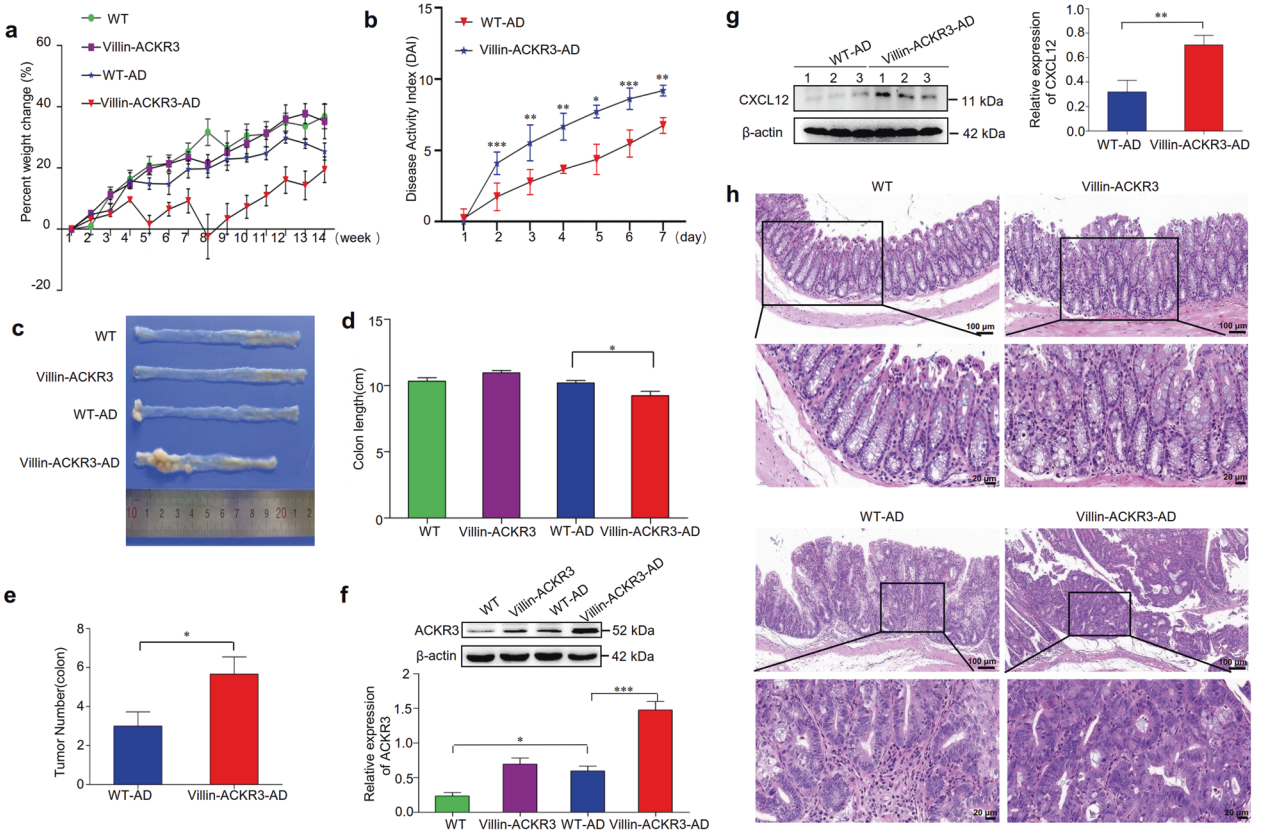

Fig. 2 Increased severity of colorectal cancer in Villin-ACKR3 mice. a Body weight changes. $n = 6$. **b** Disease activity index score (DAI) during the third DSS cycle: WT-AD (red), Villin-ACKR3-AD (blue). $n = 6$. **c** Images of colorectal cancer and (**d**) colorectal length. $n = 6$. **e** Colorectal tumours in WT-AD and Villin-ACKR3-AD mice. $n = 6$. **f** Levels of ACKR3 in colorectal cancer cells from WT, Villin-ACKR3, WT-AD, and Villin-ACKR3-AD mice; $n = 3$. **g** Western blotting of CXCL12 in CRC tissues of WT-AD and Villin-ACKR3-AD mice. $n = 3$. 1, 2, 3 represent three mice. **h** H&E-stained cancer tissues in mice. Upper images 10×, lower images 40×. The boxed region in each top panel is magnified and shown in the corresponding bottom panel. (10×) scale bar: 100 μm, (40×) scale bar: 20 μm. $n = 3$. $^*P < 0.05$, $^{**}P < 0.01$, $^{***}P < 0.001$ between Villin-ACKR3 mice and their WT littermates. WT-AD: wild mice exposed to AOM/DSS. Villin-ACKR3-AD: Villin-ACKR3 mice exposed to AOM/DSS.

arr1 might interact with NOLC1. As expected, an interaction of β-arr1 with NOLC1 was identified in CXCL12-treated HCT116 cells. The Co-IP assay showed an interaction of β-arr1 with NOLC1 in HCT116 cells with activated ACKR3 (Fig. 3g, i–ii). Since NOLC1 levels vary during the cell cycle [24], we identified an interaction of β-arr1 with NOLC1 more obviously in interphase and telophase than in prophase and metaphase (Fig. 3h). Conversely, in cancer cells with silenced ACKR3 (Fig. 3i), the interaction of β-arr1 with NOLC1 was blocked (Fig. 3i-ii, arrows). These results indicated that nuclear NOLC1 was further activated by ACKR3-activated β-arr1.

ACKR3-activated β-arr1 activated NOLC1 in the nucleus, and activated NOLC1 further translocated into the nucleolus to promote fibrillarin levels

NOLC1 is a phosphorylated nucleolar protein that functions as a regulator of RNA polymerase I. However, little is known about its roles in colonic tumorigenesis. The Cancer Genome Atlas (TCGA) reported high levels of NOLC1 in CRCs (Fig. 4a). Our results showed an increase in NOLC1 in CRC grown in Villin-ACKR3 mice (Fig. 4b) as well as human colon cancer tissues (Fig. 4c). We performed an immunofluorescence assay to mark the colocalization of NOLC1 with fibrillarin, rRNA methyltransferase, and UBF1, nucleolar transcription factor 1, in the nucleolus. NOLC1 was precisely identified in the nucleolus of cancer cells (Fig. 4d). Conversely, NOLC1 was not identified in the nucleolus of cancer cells with knockdown of β-arr1 (Fig. 4e) or ACKR3 (Fig. 4f). These results indicated that ACKR3-activated β-arr1 activated NOLC1 in the nucleus and that activated NOLC1 further translocated into the nucleolus to promote fibrillarin levels. HCT116 cells with silencing of β-arr1 failed to respond to CXCL12-stimulated cancer cell growth, thus suggesting the role of ACKR3-activated β-arr1-NOLC1-fibrillarin signalling in colonic tumorigenesis (Fig. 4g).

β-arr1-activated NOLC1 promoted the synthesis of ribosomal biogenesis rRNA

We analysed the level of AgNOR protein to evaluate the role of β-arr1-activated NOLC1 in promoting the synthesis of rRNA in ribosome biogenesis. A deeper and wider staining of AgNOR proteins was identified in the nucleus of cancer cells from Villin-ACKR3 mice than in those from WT mice (Fig. 5a). To illustrate the role of NOLC1 in the nucleolus, we employed a cell model in which NOLC1 was silenced to analyse the levels of rRNA synthesis during ribosome biogenesis. We designed three types of siRNAs to target NOLC1. The levels of NOLC1 were reduced by 51.2%, 49.7%, and 65.1% in si1-, si2-, and si3-treated HCT116 cells, respectively (Fig. 5b). Silencing NOLC1 with si3 resulted in a reduction in nucleoli (Fig. 5c). We then analysed the levels of precursor rRNA 45 S, 36 S, and 32 S rRNA by RT–qPCR assay. As shown in Fig. 5d, the levels of pre-rRNA 45 S, 36 S, and 32 S were significantly downregulated in the cells with silenced NOLC1 (siNOLC1 cells) compared with WT cells. These results indicated that silencing NOLC1 resulted in a reduction in rRNA synthesis. We further analysed the nucleolar sizes of cells with NOLC1 silencing under transmission electron microscopy. Silencing of the NOLC1 gene resulted in a smaller nucleolus than that in control cells (Fig. 5e). Western blotting assays demonstrated a higher level of nucleolar

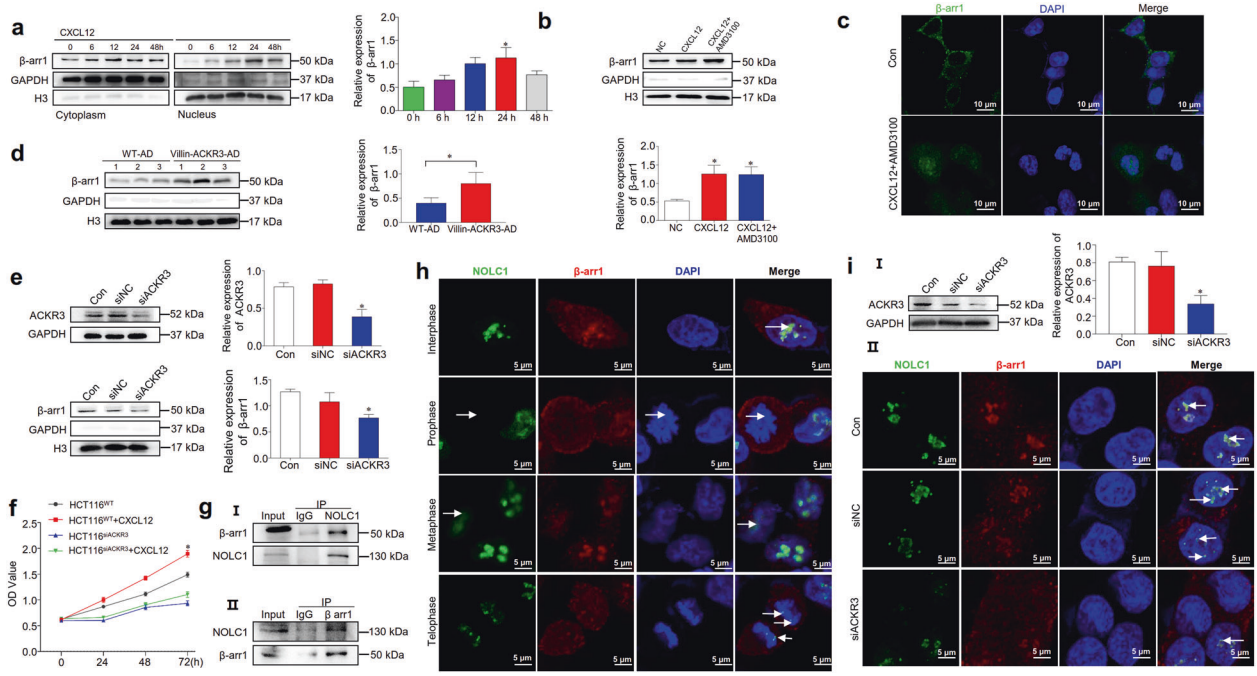

Fig. 3 Activation of ACKR3 induced the recruitment of β-arr1 to the nucleus and further interaction with NOLC1. a HCT116 cells exposed to CXCL12 for increasing times. Cytoplasmic and nuclear extracts were subjected to Western blotting to analyse β-arr1 expression. $n = 3$. **b** HCT116 cells were exposed to CXCL12 and CXCL12 + AMD3100, and nuclear extracts were subjected to Western blotting to analyse β-arr1 expression. $n = 3$. **c** Immunofluorescence staining was used to analyse the localisation of β-arr1 in HCT116 cells exposed to CXCL12 and AMD3100. Scale bar: 10 μm. **d** Western blotting showed β-arr1 expression in the nucleus of colorectal cancer cells from Villin-ACKR3-AD and WT-AD mice. 1, 2, 3 represent three mice. **e** Knockdown of ACKR3 downregulated the levels of β-arr1. $n = 3$. **f** An MTT assay was used to estimate the growth of WT HCT116 cells and HCT116^{siACKR3} cells exposed to CXCL12. **g** A Co-IP assay identified an interaction between β-arr1 and NOLC1 in HCT116 cells exposed to CXCL12. **h** Immunofluorescence analysis showed variation in NOLC1 and β-arr1 colocalization during the cell cycle of HCT116 cells exposed to CXCL12. Scale bar: 5 μm. **i** Western blotting was used to analyse ACKR3 levels in HCT116 cells with silenced ACKR3 (I). Silencing ACKR3 blocked the interaction of β-arr1 with NOLC1 (II, arrows). Scale bar: 5 μm. Arrows show the colocalization between NOLC1 and β-arr1. *$P < 0.05$ between WT and siACKR3 cells.

NOLC1 in colon cancer cells in Villin-ACKR3-AD mice than in WT-AD mice. These cancer cells with elevated NOLC1 demonstrated a higher level of POLR1A (RPA194), the largest subunit of RNA Pol I, and a higher level of UBF1, the transcription initiation factor of rRNA transcription, in Villin-ACKR3-AD mice than in WT mice (Fig. 5f). These results indicated that ACKR3-activated nucleolar NOCL1 is associated with the increased synthesis of rRNA during ribosome biogenesis. HCT116 cells with silenced NOCL1 failed to respond to CXCL12-stimulated cancer cell growth, suggesting the role of β-arr1-activated NOLC1 in promoting the synthesis of rRNA in ribosome biogenesis (Fig. 5g).

The interaction of NOLC1 with nucleolar fibrillarin led to an increase in rRNA transcription

Fibrillarin plays an important role in tumorigenesis by increasing rRNA transcription [24]. As β-arr1-activated NOLC1 promoted fibrillarin levels, we next explored the roles of activated fibrillarin in the synthesis of rRNA. Analysis of the GEPIA database indicated a correlation of nucleolar NOLC1 to fibrillarin in CRC tissues (correlation coefficient $R = 0.4$, Fig. 6a). Further immunofluorescence analysis indicated a strong colocalization of NOLC1 with fibrillarin in the nucleolus of HCT116 cells (Fig. 6b). Western blotting analysis showed a higher fibrillarin level in Villin-ACKR3 mice than in WT mice (Fig. 6c). Conversely, knockdown of NOLC1 resulted in a decrease in fibrillarin, indicating that fibrillarin was a transporter of activated NOLC1 (Fig. 6d). Co-IP analysis showed an interaction between NOLC1 and fibrillarin (Fig. 6e–i) in CRC cells of Villin-ACKR3 mice but not in colonic mucosal cells of WT-AD mice (Fig. 6e–ii). These results indicated that activated NOLC1 promoted the fibrillarin level in the nucleolus; accordingly, elevated fibrillarin played an important role in rRNA transcription in CRC cells of Villin-ACKR3 mice (Fig. 6f).

DISCUSSION

It is known that, as an atypical GPCR, targeting ACKR3 does not lead to the typical G-protein-coupled receptor-mediated calcium mobilisation and chemotaxis but rather the recruitment of β-arrestins and the internalisation of GPCR [25]. ACKR3 has been considered a scavenger receptor and decoy receptor [5, 6]. ACKR3 is upregulated in various inflammatory cells and malignant cells. To date, we do not have a complete understanding of how activated ACKR3 signalling is integrated to induce tumorigenesis. Since Villin-ACKR3 mice developed more exacerbated CRC than Villin-CXCR4 mice, we hypothesise that ACKR3 plays a crucial role independent of CXCR4.

To unveil the mechanism of activated ACKR3 in colorectal tumorigenesis, we first explored how activated ACKR3 signalling is translocated into the nucleus. It is noted that GPCRs can interact with β-arrestins (β-arr1 and β-arr2) to function as scaffolds for multiple kinases that connect GPCRs to effector pathways. These complex signalling networks and interactions are facilitated by a conformational change in β-arrs that is thought to occur upon binding to a phosphorylated GPCR [5]. Previous reports indicated that activation of ACKR3 could recruit β-arr2 into the nucleus through the AKT and ERK1/2 signalling pathways [6, 26, 27]. Since β-arr2 has a NES in its C-terminus, this specific NES excludes it from its sustained presence in the nucleus [28]. In this study, we revealed that activation of ACKR3 could induce nuclear translocation of β-arr1 but not β-arr2 into the nucleus. Importantly,

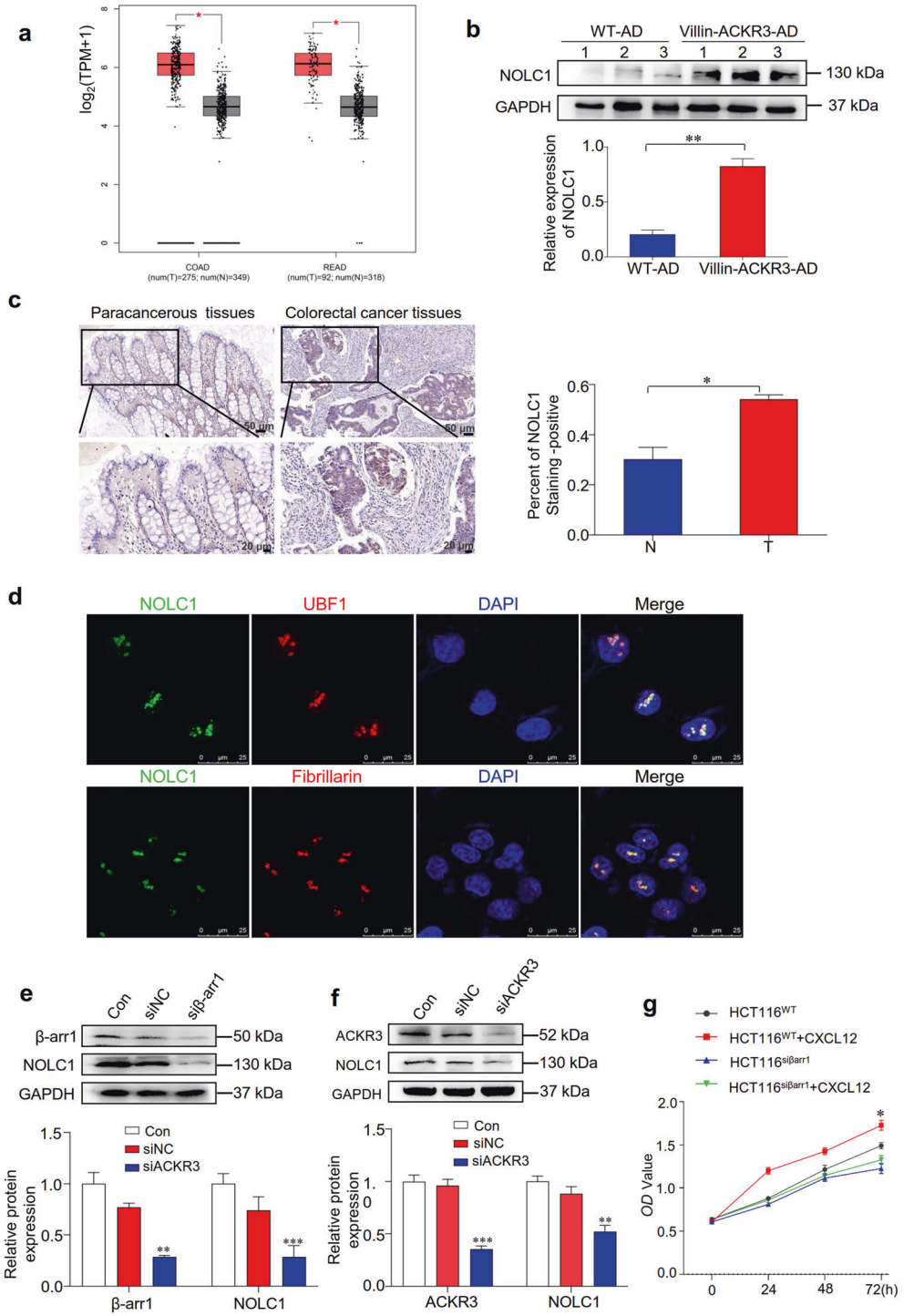

Fig. 4 The interaction of β-arr1 with NOLC1 led to an increase in NOLC1 in the nucleolus. a Levels of NOLC1 in CRC in TCGA datasets. Differences were seen in NOLC1 levels between colonic tumour (orange) and paracancerous tissues (grey). COAD: colon adenocarcinoma, READ: rectum adenocarcinoma. Log2(TPM + 1) used for log-scale. The calculated means ± SEM are represented by bars and whiskers. **b** Western blotting of NOLC1 in Villin-ACKR3-AD and WT-AD mice. 1, 2, 3 represent three mice. **c** Level of NOLC1 in CRC tissues (T) and paired noncancer tissues (N). Upper images 20×, lower images 40×. The boxed region in each top panel is magnified and shown in the corresponding bottom panel. (20×) Scale bar: 50 μm, (40×) Scale bar: 20 μm. $n = 5$. **d** NOLC1 was localised to the nucleolus. Costaining of NOLC1, fibrillarin and UBF1 in HCT116 cells. Scale bar: 25 μm. $n = 3$. **e** Knockdown of β-arr1 downregulated NOLC1 levels in CRC cells. $n = 3$. **f** Western blotting of NOLC1 levels in cancer cells with ACKR3 knockdown. **g** The MTT assay estimated the growth of WT-type HCT116 cells and HCT116$^{si\beta arr1}$ cells exposed to CXCL12. $^{*}P < 0.05$, $^{**}P < 0.01$, $^{***}P < 0.001$ between WT and siβ-arr1 cells.

ACKR3-induced β-arr1 interacted with NOLC1, the most highly nuclear phosphoprotein, to form the β-arr1-NOLC1 complex.

How was NOLC1 identified as the downstream effector of ACKR3-induced β-arr1? We first searched for clues about the interaction related to nuclear β-arr1 in the Hitpredict database. An interesting link between β-arr1 and NOLC1 was found in the database. Previously, NOLC1 was identified as a nuclear localisation signal-binding protein and functions as a chaperone for

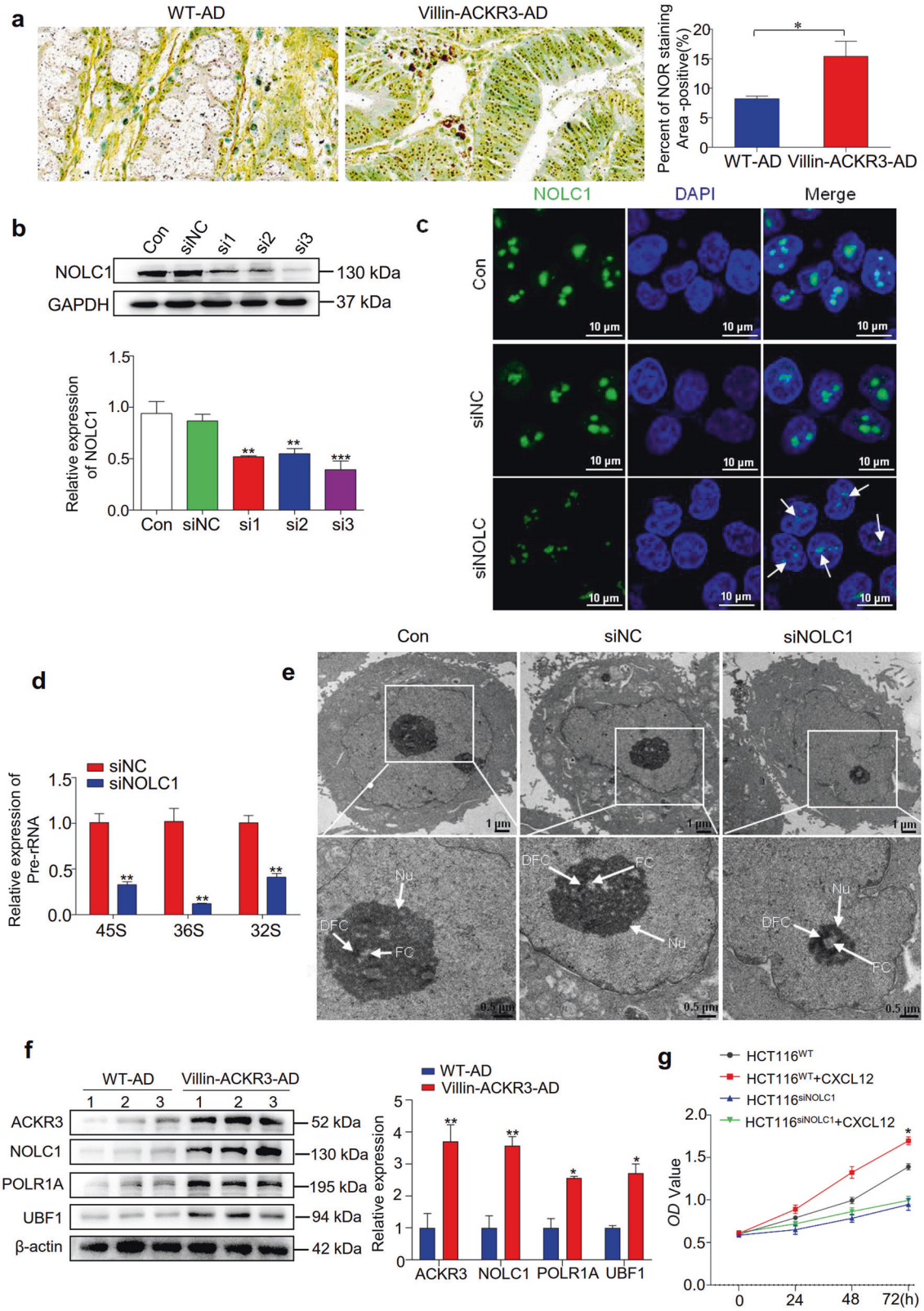

Fig. 5 Upregulating NOLC1 by ACKR3-activated β-arr1 increased the synthesis of rRNA during ribosome biogenesis. a AgNOR staining of colonic tissues in WT-AD and Villin-ACKR3-AD mice. Scale bar: 10 μm. $n = 6$. $^{*}P < 0.05$ between WT-AD and Villin-ACKR3-AD. **b** Western blotting of NOLC1 in HCT116 cells with ACKR3 knockdown. $n = 3$. **c** Immunofluorescence staining of NOLC1 in cancer cells. Scale bar: 10 μm. $n = 3$. **d** Real-time PCR analysis of 45 S, 36 S, and 32 S pre-RNA in HCT116 cells. $n = 3$. (**e**) Transmission electron microscopy showed the nucleolus in HCT116 cells (Con), siNC cells (siNC), and NOLC1-silenced cells (siNOLC1). $n = 3$. **f** Western blotting of ACKR3, NOLC1, POLR1A and UBF1 levels in colonic tissues of WT-AD and Villin-ACKR3-AD mice. 1, 2, 3 represent three mice. $n = 3$. DFC, FC and nucleolus are indicated with arrows. **g** The MTT assay estimated the growth of WT-type HCT116 cells and HCT116^{siNOLC1} cells exposed to CXCL12. $^{*}P < 0.05$, $^{**}P < 0.01$, $^{***}P < 0.001$ between WT cells and siNOLC1 cells. DFC Dense Fibrillar Component. FC Fibrillar Center. Nu Nucleolus.

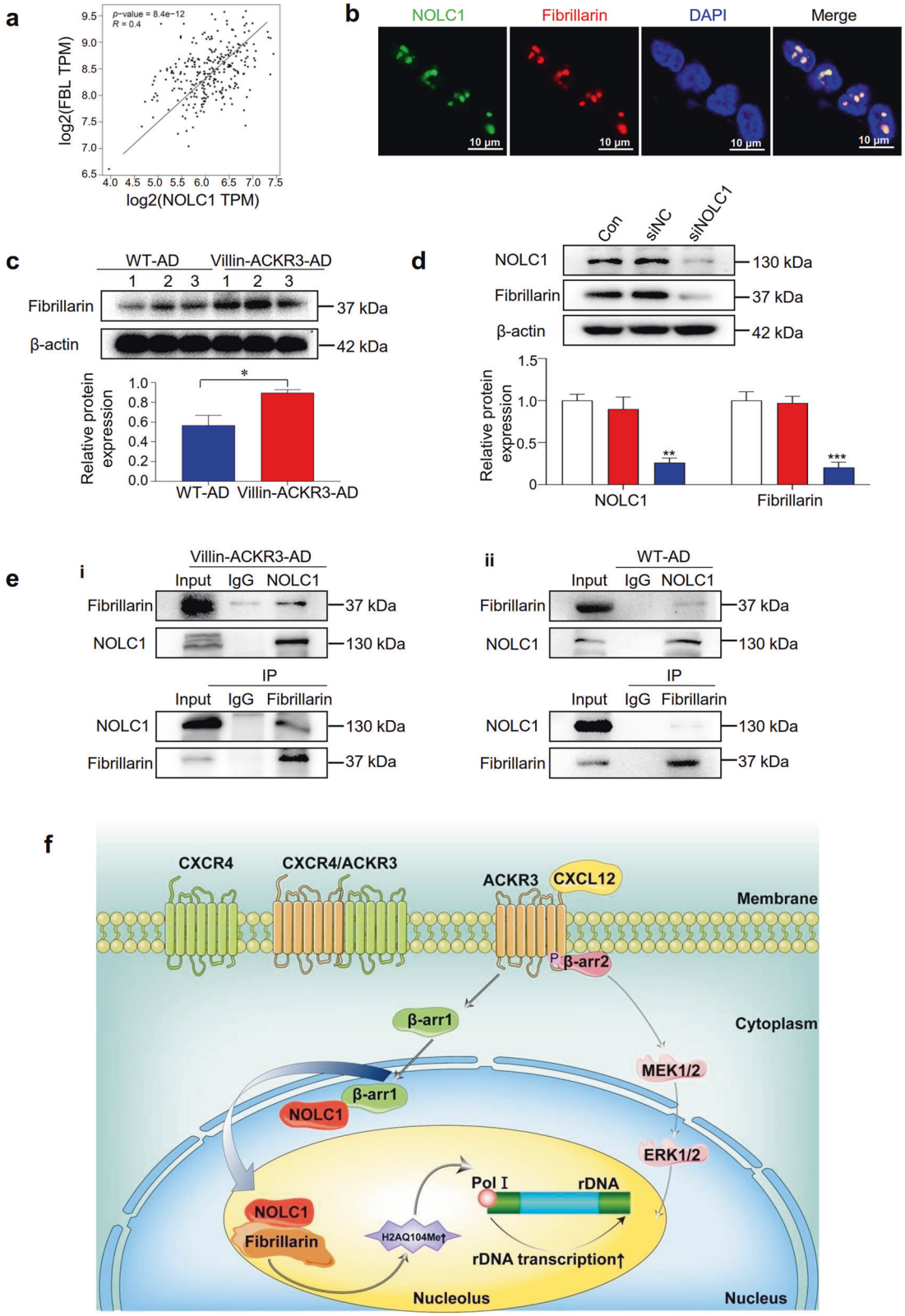

Fig. 6 The interaction of NOLC1 with Fibrillarin led to an increase in Fibrillarin and Fibrillarin-promoted rRNA transcription. a Correlation analysis of NOLC1 to fibrillarin in colorectal cancer tissues in the GEPIA database. **b** Immunofluorescence staining showed an interaction of NOLC1 with fibrillarin in the nucleolus. Scale bar: 10 μm. $n = 3$. **c** Western blotting analysis of fibrillarin levels in colorectal cancer cells from Villin-ACKR3-AD and WT-AD mice. 1, 2, 3 represent three mice. $n = 3$. (**d**) Western blotting analysis of NOLC1 and fibrillarin in WT and siNOLC1 HCT116 cells. $n = 3$. **e** Co-IP of colorectal cancer cells in Villin-ACKR3-AD mice showed an interaction between NOLC1 and Fibrillarin (Fig. 6e–I) but not in colonic mucosal cells in WT-AD mice (Fig. 6e–II). **f** Proposed mechanism by which ACKR3 is upregulated in colorectal tumorigenesis. Upregulating ACKR3 induced nuclear translocation of β-arr1, leading to an interaction of NOLC1 and resulting in fibrillarin-induced rRNA transcription of ribosome biogenesis. $^{*}P < 0.05$, $^{**}P < 0.01$, $^{***}P < 0.001$ between Villin-ACKR3-AD and WT-AD mice.

shuttling between the nucleolus and cytoplasm. However, the mechanisms and biological functions remain largely unknown, and its roles in the development of tumorigenesis are largely contradictory among reports [29–31]. Since NOLC1 was upregulated in interphase and telophase, it is thus suggested that the interaction of nuclear β-arr1 with NOLC1 might play the role of overproliferation in cancer cells. However, there were some contradictory reports that nuclear NOLC1 increased the percentage of cells in the G_0/G_1 phase [32]. Our results revealed that the ACKR3-induced interaction of β-arr1 with NOLC1 occurred in interphase and telophase but not in prophase or metaphase. These results indicated that the interaction of activated β-arr1 with NOLC1 resulted in the upregulation of NOLC1 in the nucleolus.

NOLC1 was identified as the downstream effector of activated β-arr1. High ribosome biogenesis is associated with the key process of overproliferation and tumorigenesis in many types of cancer cells [33]. Ribosome biogenesis is actually a complex and well-orchestrated cellular process [34]. The regulation of ribosome biogenesis, particularly the production of rRNA, is a critical aspect of cell growth control [35]. The nucleolus, a nuclear subcompartment where ribosomal RNA is synthesised and assembled into ribosomal subunits, is the main site of ribosome biogenesis [36]. It is a dynamic organelle subject to inputs from growth signalling pathways, nutrients, and stress, whose size correlates with rRNA synthesis [37]. In the nucleolus, NOLC1 interacts with RNA polymerase I, leading to the regulation of rRNA transcription, perhaps by linking RNA Pol I transcription with pre-rRNA processing. NOLC1 also plays an essential role in rDNA transcription and further induces the synthesis of rRNA in ribosome biogenesis [38]. Thus, ribosome biogenesis is identified as the downstream effector of nuclear NOLC1. In the present study, we found that CRC grown in Villin-ACKR3 mice demonstrated elevated ribosome biogenesis, and conversely, knockdown of NOLC1 resulted in a decrease in pre-rRNA and smaller nucleolar size in cancer cells. Activated NOLC1 was found to further interact with fibrillarin in the process of tumorigenesis. CRC developed in Villin-ACKR3 mice demonstrated an interaction of NOLC1 with fibrillarin in the nucleolus. Conversely, knockdown of NOLC1 downregulated the expression levels of fibrillarin in the nucleolus. As a highly conserved nucleolus protein, fibrillarin plays a crucial role in the regulation of ribosome biogenesis by promoting the methylation of ribosomal RNAs and rDNA histones [39]. Accordingly, fibrillarin might be a downstream signalling target of activated NOLC1. However, the mechanism of NOLC1-activated fibrillarin in ribosome biogenesis has not been fully investigated. A report indicated that enhanced fibrillarin might increase rRNA transcription by activating RNA Pol I methylation in H2AQ104 [40–42]. In CRC of Villin-ACKR3 mice, ACKR3-activated NOLC1 promoted nuclear fibrillarin levels; accordingly, enhanced fibrillarin functions in the upregulation of ribosome biogenesis by promoting the methylation of ribosomal RNAs and rDNA histones.

Overall, ACKR3 promotes colorectal tumorigenesis through the perturbation of rRNA biogenesis by the nuclear β-arr1-induced interaction of NOLC1 with fibrillarin. We envision that future approaches to treat CRC should use ACKR3 inhibitors to block ACKR3-activated NOLC1 and fibrillarin in the nucleolus.

ACKNOWLEDGEMENTS

This work was supported by Beijing Natural Science Foundation (7212149/7222253) and National Natural Science Foundation of China (82173841/81872884/81973350/81772637/82002574).

AUTHOR CONTRIBUTIONS

SXC conceived the project. JY, YNL and TP performed the experiments of molecular mechanisms and conducted animal studies. SHW provided clinical samples and pathological analysis. RRM performed statistical analysis. XJQ wrote the paper, which was edited by all authors.

ADDITIONAL INFORMATION

Supplementary information The online version contains supplementary material available at https://doi.org/10.1038/s41401-022-00901-x.

Competing interests: The authors declare no competing interests.

REFERENCES

1. Huynh C, Dingemanse J, Schwabedissen HEM, Sidharta PN. Relevance of the CXCR4/CXCR7-CXCL12 axis and its effect in pathophysiological conditions. Pharmacol Res. 2020;161:105092.
2. Stacer AC, Fenner J, Cavnar SP, Xiao A, Zhao S, Chang SL, et al. Endothelial CXCR7 regulates breast cancer metastasis. Oncogene. 2016;35:1716–24.
3. Bachelerie F, Graham GJ, Locati M, Mantovani A, Murphy PM, Nibbs R, et al. New nomenclature for atypical chemokine receptors. Nat Immunol. 2014;15:207–8.
4. Cancellieri C, Vacchini A, Locati M, Bonecchi R, Borroni EM. Atypical chemokine receptors: from silence to sound. Biochem Soc Trans. 2013;41:231–6.
5. Meyrath M, Szpakowska M, Zeiner J, Massotte L, Merz MP, Benkel T, et al. The atypical chemokine receptor ACKR3/CXCR7 is a broad-spectrum scavenger for opioid peptides. Nat Commun. 2020;11:3033.
6. Luker KE, Lewin SA, Mihalko LA, Schmidt BT, Winkler JS, Coggins NL, et al. Scavenging of CXCL12 by CXCR7 promotes tumor growth and metastasis of CXCR4-positive breast cancer cells. Oncogene. 2012;31:4750–8.
7. Sanchez-Martin L, Sanchez-Mateos P, Cabanas C. CXCR7 impact on CXCL12 biology and disease. Trends Mol Med. 2013;19:12–22.
8. Yan Y, Su J, Zhang Z. The CXCL12/CXCR4/ACKR3 response axis in chronic neurodegenerative disorders of the central nervous system: therapeutic target and biomarker. Cell Mol Neurobiol. 2021; https://doi.org/10.1007/s10571-021-01115-1.
9. Gutjahr JC, Crawford KS, Jensen DR, Naik P, Peterson FC, Samson GPB, et al. The dimeric form of CXCL12 binds to atypical chemokine receptor 1. Sci Signal. 2021;14:eabc9012.
10. Jiang C, Li R, Xiu C, Ma X, Hu H, Wei L, et al. Upregulating CXCR7 accelerates endothelial progenitor cell-mediated endothelial repair by activating Akt/Keap-1/Nrf2 signaling in diabetes mellitus. Stem Cell Res Ther. 2021;12:264.
11. Song S, Liu B, Habibie H, van den Bor J, Smit MJ, Gosens R, et al. D-dopachrome tautomerase contributes to lung epithelial repair via atypical chemokine receptor 3-dependent Akt signaling. EBioMedicine. 2021;68:103412.
12. Correia AL, Guimaraes JC, Auf der Maur P, De Silva D, Trefny MP, Okamoto R, et al. Hepatic stellate cells suppress NK cell-sustained breast cancer dormancy. Nature. 2021;594:566–71.
13. Giallongo C, Dulcamare I, Tibullo D, Del Fabro V, Vicario N, Parrinello N, et al. CXCL12/CXCR4 axis supports mitochondrial trafficking in tumor myeloma microenvironment. Oncogenesis. 2022;11:6.
14. Song ZY, Wang F, Cui SX, Gao ZH, Qu XJ. CXCR7/CXCR4 heterodimer-induced histone demethylation: a new mechanism of colorectal tumorigenesis. Oncogene. 2019;38:1560–75.
15. Scott MGE, Rouzic EL, Perianin A, Pierotti V, Enslen H, Benichou S, et al. Differential nucleocytoplasmic shuttling of beta-arrestins. Characterization of a leucine-rich nuclear export signal in beta-arrestin2. J Biol Chem. 2002;277:37693–701.
16. Meier UT. Comparison of the rat nucleolar protein Nopp140 with its Yeast Homolog SRP40. J Biol Chem. 1996;271:19376–84.
17. Kim YK, Jin Y, Vukoti KM, Park JK, Kim EE, Lee KJ, et al. Purification and characterization of human nucleolar phosphoprotein 140 expressed in *Escherichia coli*. Protein Expr Purif. 2003;31:260–4.
18. Yi Y, Li Y, Meng Q, Li Q, Li F, Lu B, et al. A PRC2-independent function for EZH2 in regulating rRNA 2′-O methylation and IRES-dependent translation. Nat Cell Biol. 2021;23:341–54.
19. Bryant CJ, McCool MA, Abriola L, Surovtseva YV, Baserga SJ. A high-throughput assay for directly monitoring nucleolar rRNA biogenesis. Open Biol. 2022;12:210305.
20. Zhang YH, Shi WN, Wu SH, Miao RR, Sun SY, Luo DD, et al. SphK2 confers 5-fluorouracil resistance to colorectal cancer via upregulating H3K56ac-mediated DPD expression. Oncogene. 2020;39:5214–27.
21. Deng QD, Lei XP, Zhong YH, Chen MS, Ke YY, Li Z, et al. Triptolide suppresses the growth and metastasis of non-small cell lung cancer by inhibiting β-catenin-mediated epithelial-mesenchymal transition. Acta Pharmacol Sin. 2021;42:1486–97.
22. Trerè D. AgNOR staining and quantification. Micron. 2000;31:127–31.
23. Pai CY, Chen HK, Sheu HL, Yeh NH. Cell-cycle-dependent alterations of a highly phosphorylated nucleolar protein p130 are associated with nucleologenesis. J Cell Sci. 1995;108:1911–20.

24. Duchemin A, O'Grady T, Hanache S, Mereau A, Thiry M, Wacheul L, et al. DHX15-independent roles for TFIP11 in U6 snRNA modification, U4/U6.U5 tri-snRNP assembly and pre-mRNA splicing fidelity. Nat Commun. 2021; 12:6648.
25. Nguyen HT, Reyes-Alcaraz A, Yong HJ, Nguyen LP, Park HK, Inoue A, et al. CXCR7: a beta-arrestin-biased receptor that potentiates cell migration and recruits beta-arrestin2 exclusively through Gbetagamma subunits and GRK2. Cell Biosci. 2020;10:134.
26. Charest PG, Terrillon S, Bouvier M. Monitoring agonist-promoted conformational changes of beta-arrestin in living cells by intramolecular BRET. EMBO Rep. 2005;6:334–40.
27. Min K, Yoon HJ, Park JY, Baidya M, Dwivedi-Agnihotri H, Maharana J, et al. Crystal structure of beta-Arrestin 2 in complex with CXCR7 phosphopeptide. Structure. 2020;28:1014–23.
28. Becker JH, Gao Y, Soucheray M, Pulido I, Kikuchi E, Rodríguez ML, et al. CXCR7 reactivates ERK signaling to promote resistance to EGFR kinase inhibitors in NSCLC. Cancer Res. 2019;79:4439–52.
29. Lin L, Han MM, Wang F, Xu LL, Yu HX, Yang Y, et al. CXCR7 stimulates MAPK signaling to regulate hepatocellular carcinoma progression. Cell Death Dis. 2014;5:e1488.
30. Wang P, Wu Y, Ge X, Ma L, Pei G. Subcellular localization of beta-arrestins is determined by their intact N domain and the nuclear export signal at the C terminus. J Biol Chem. 2003;278:11648–53.
31. Hwang YC, Lu TY, Huang DY, Kuo YS, Kao CF, Yeh NH, et al. NOLC1, an enhancer of nasopharyngeal carcinoma progression, is essential for TP53 to regulate MDM2 expression. Am J Pathol. 2009;175:342–54.
32. Huang H, Li T, Chen M, Liu F, Wu H, Wang J, et al. Identification and validation of NOLC1 as a potential target for enhancing sensitivity in multidrug resistant non-small cell lung cancer cells. Cell Mol Biol Lett. 2018;23:54.
33. Yuan F, Zhang Y, Ma L, Cheng Q, Li G, Tong T, et al. Enhanced NOLC1 promotes cell senescence and represses hepatocellular carcinoma cell proliferation by disturbing the organization of nucleolus. Aging Cell. 2017;16:726–37.
34. Yuan F, Li G, Tong T. Nucleolar and coiled-body phosphoprotein 1 (NOLC1) regulates the nucleolar retention of TRF2. Cell Death Discov. 2017;3:17043.
35. Penzo M, Montanaro L, Trere D, Derenzini M. The ribosome biogenesis-cancer connection. Cells. 2019;8:8010055.
36. Pelletier J, Thomas G, Volarević S. Ribosome biogenesis in cancer: new players and therapeutic avenues. Nat Rev Cancer. 2018;18:51–63.
37. Mayer C, Grummt I. Ribosome biogenesis and cell growth: mTOR coordinates transcription by all three classes of nuclear RNA polymerases. Oncogene. 2006;25:6384–91.
38. Grummt I. The nucleolus-guardian of cellular homeostasis and genome integrity. Chromosoma. 2013;122:487–97.
39. Boulon S, Westman BJ, Hutten S, Boisvert FM, Lamond AI. The nucleolus under stress. Mol Cell. 2010;40:216–27.
40. Meier UT. The many facets of H/ACA ribonucleoproteins. Chromosoma. 2005;114:1–14.
41. Hassouni BE, Sarkisjan D, Vos JC, Giovannetti E, Peters GJ. Targeting the ribosome biogenesis key molecule Fibrillarin to avoid chemoresistance. Curr Med Chem. 2019;26:6020–32.
42. Tessarz P, Santos-Rosa H, Robson SC, Sylvestersen KB, Nelson CJ, Nielsen ML, et al. Glutamine methylation in histone H2A is an RNA-polymerase-I-dedicated modification. Nature. 2014;505:564–8.